

Recent τ physics studies at *BABAR*

F. F. Wilson^a (on behalf of the *BABAR* Collaboration)

^aRutherford Appleton Laboratory, Chilton, Didcot,
Oxford, OX11 0QS, UK

Contribution to the International Workshop on e^+e^- collisions from Φ to Ψ , 27th February to 2nd March 2006,
Novosibirsk, Russia.

Recent results from τ physics studies at *BABAR* are presented with an emphasis on hadronic decays and lepton flavor violation studies.

1. τ physics studies at *BABAR*

The *BABAR* and Belle B -meson Factories also produce copious numbers of τ decays. The *BABAR* detector (described in detail in Ref. [1]) operates at the Stanford Linear Accelerator Center the PEP-II asymmetric-energy e^+e^- storage ring. The luminosity is recorded at center-of-mass (CM) energies (\sqrt{s}) of 10.58 GeV and 10.54 GeV. The luminosity-averaged a cross section for τ pairs for these CM energies is $\sigma_{\tau\tau} = (0.89 \pm 0.02)$ nb which is of the same order as the the $b\bar{b}$ cross section $\sigma_{b\bar{b}} \sim 1.05$ nb.

The analyses follow a similar strategy. Each analysis looks for the production of τ pairs where one of the τ decays to either a 1-prong ($\tau^- \rightarrow l^- \nu_\tau \nu_\mu, \pi^- \nu_\tau, \rho^- \nu_\tau$) or 3-prong ($\tau^- \rightarrow 2h^- h^+ (n\pi^0) \nu_\tau$) final state which covers roughly 99% of the τ branching fraction. The event is divided into two hemispheres in the CM frame based on the plane perpendicular to the thrust axis from the tracks in the event. Each hemisphere is assumed to contain the decay products of a single τ lepton. The analysis procedure selects events with 1-prong or 3-prong in one hemisphere (tag hemisphere) and tracks from the other τ in the other hemisphere (signal hemisphere). A cut on the event thrust is applied to reject light quark production $e^+e^- \rightarrow q\bar{q}$ ($q = \{u, d, s, c, b\}$) and $b\bar{b}$ backgrounds. Particle identification is applied to the tracks and the total event charge is

required to be zero.

The τ is reconstructed from tracks and neutral deposits not in the the tag hemisphere according to the analysis under consideration. Charged particles are required to have a minimum momentum and come from the beam spot. Tracks coming from photon conversions are rejected. Neutral energy deposits must be consistent with the pion and criteria are applied to reject photons where necessary.

The backgrounds come from a number of sources. Other τ decays where a particle is missed or added can be eliminated by careful construction of the signal mode. Bhabhas and di-muon events can be removed through criteria based on the event thrust, colinearity of the tracks in the CM frame, the momentum of the two leptons in the CM frame and the reconstructed τ mass. Hadronic events from $q\bar{q}$ production can be suppressed through the event thrust, the topology of the decay and an excess of neutral energy. Two photon events have large missing energy and small transverse momentum that can be used to reject them.

Monte Carlo (MC) simulation is used to evaluate the background contamination and selection efficiency. The methods for extracting the signal yield vary depending on the analysis. Some analyses use a cut-based approach while others use a Maximum Likelihood (ML) technique. The systematic errors on the signal efficiencies in-

clude contributions from uncertainties in the reconstruction efficiency of charged tracks and neutral deposits; the uncertainty associated with the particle identification on the signal and tag side; the luminosity measurement and the τ pair cross-section determination; and the uncertainty on decay branching ratios.

Unless otherwise stated, the data sample consists of an integrated luminosity of $\mathcal{L} = 210.6 \text{ fb}^{-1}$ recorded at a $\sqrt{s} = 10.58 \text{ GeV}$, and 21.6 fb^{-1} recorded at $\sqrt{s} = 10.54 \text{ GeV}$.

2. Hadronic decays of the τ

Tau decays to one and three charged hadrons have been used to test the Standard Model, measure the masses of the τ^- and ν_τ , study the properties of low-mass resonances, test CP violation in the lepton sector, and search for new physics. The high-statistics sample of τ pair events collected by the *BABAR* Collaboration allows detailed studies of rare decays of the τ lepton to states with multiple charged and neutral hadrons

2.1. $\tau^- \rightarrow 3h^- 2h^+ \nu_\tau$ decays [2]

The analysis procedure selects events with one electron or muon track in the tag hemisphere and five tracks in the signal hemisphere. Events are retained if they pass selection criteria based on the magnitude of the event thrust (T) and the ratio p_T/E_{missing} .

A total of 20920 and 13929 events are selected when an electron or muon, respectively, are identified in the tag hemisphere. The efficiencies are $(4.71 \pm 0.05)\%$ and $(3.03 \pm 0.04)\%$ in the electron and muon samples, respectively. The branching fraction of the τ leptonic decay mode is incorporated into the selection efficiency. The background percentages in the electron and the muon tag samples estimated from the Monte Carlo (MC) simulation are $(20.6 \pm 2.0)\%$ and $(21.7 \pm 2.1)\%$, respectively. The branching fraction of the $\tau^- \rightarrow 3\pi^- 2\pi^+ \nu_\tau$ decay is found to be $(8.53 \pm 0.06 \pm 0.42) \times 10^{-4}$ and $(8.73 \pm 0.07 \pm 0.48) \times 10^{-4}$ for the data selected by the electron and muon tags, respectively. The value of the branching fraction is in good agreement with the Particle Data Group average of $(8.2 \pm 0.6) \times 10^{-4}$.

Fig. 1 shows the mass of h^+h^- pair combinations where the shoulder at $0.77 \text{ GeV}/c^2$ suggests a strong contribution from the ρ resonance. The discrepancy between Tauola MC [3], which uses a phase space distribution for $\tau^- \rightarrow 3\pi^- 2\pi^+ \nu_\tau$, and the data can be clearly seen.

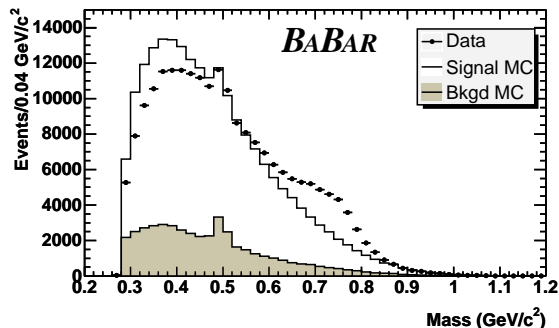


Figure 1. Reconstructed mass of h^+h^- pairs in the five tracks in the signal hemisphere. The peak at $0.5 \text{ GeV}/c^2$ is due to K_S^0 mesons that are not rejected by the selection.

The data sample can also be used to study the $\tau^- \rightarrow f_1(1285)\pi^- \nu_\tau$ decay, where the $f_1(1285)$ decays into a $2\pi^- 2\pi^+$ final state. A total of 1369 ± 232 $\tau^- \rightarrow f_1(1285)\pi^- \nu_\tau$ decays are obtained from the fit. The fraction of $\tau^- \rightarrow f_1(1285)\pi^- \nu_\tau$ decays found in the $\tau^- \rightarrow 3\pi^- 2\pi^+ \nu_\tau$ sample is measured to be $(0.050 \pm 0.008 \pm 0.005)$ and the branching fraction of the $\tau^- \rightarrow f_1(1285)\pi^- \nu_\tau$ decay is calculated to be $(3.9 \pm 0.7 \pm 0.5) \times 10^{-4}$.

2.2. $\tau^- \rightarrow 4\pi^- 3\pi^+(\pi^0)\nu_\tau$ decays [4]

Events with eight charged tracks are selected with one lepton track in the tag hemisphere and 7 in the signal hemisphere with at least 6 identified as pions. The final event count is performed in the signal region $1.3 < m < 1.8 \text{ GeV}/c^2$, where m is the pseudo-mass (m) of the τ lepton: $m^2 = 2(E_{\text{beam}} - E_{7\pi})(E_{7\pi} - P_{7\pi}) + m_{7\pi}^2$.

Fig. 2 illustrates the pseudo-mass spectra of simulated signal and background contributions after the topology selection but before the pseudo-mass region selection. To determine the number of $e^+e^- \rightarrow q\bar{q}$ background events in the signal region, a fit is performed to the data events in the pseudo-mass range $1.8 < m < 2.6 \text{ GeV}/c^2$ and then extrapolated into the pseudo-mass signal region. After the final selection we observe 24 events in the data with a total number of predicted background from τ and $e^+e^- \rightarrow q\bar{q}$ events of 21.6 ± 1.2 . The efficiencies for events in the signal region for $\tau^- \rightarrow 4\pi^-3\pi^+\nu_\tau$ and $\tau^- \rightarrow 4\pi^-3\pi^+\pi^0\nu_\tau$ are $(9.4 \pm 0.1 \pm 0.6)\%$ and $(9.3 \pm 0.1 \pm 0.6)\%$.

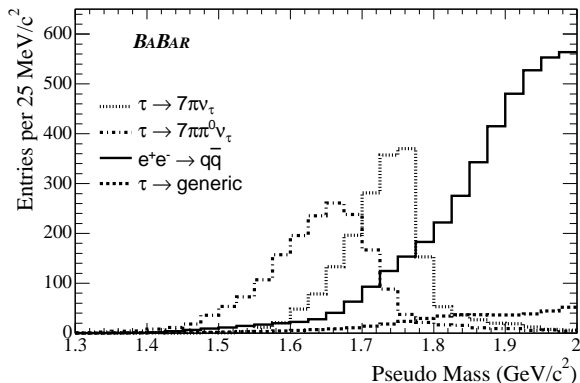


Figure 2. Pseudo mass distributions of the seven charged tracks. To display the two signal modes we assumed a branching fraction of 2×10^{-5} .

The $\tau^- \rightarrow 4\pi^-3\pi^+(\pi^0)\nu_\tau$ branching fraction is calculated from a likelihood function that accounts for uncertainties in the background and efficiency. We obtain a central value of $(0.7_{-1.3}^{+1.4}) \times 10^{-7}$ and an upper limit at 90% confidence level (CL) of $< 3.0 \times 10^{-7}$. Limits at 90% CL are also set on the exclusive decay modes $\tau^- \rightarrow 4\pi^-3\pi^+\nu_\tau$ and $\tau^- \rightarrow 4\pi^-3\pi^+\pi^0\nu_\tau$ of $< 4.3 \times 10^{-7}$ and $< 2.5 \times 10^{-7}$ respectively.

3. Lepton Flavor Violation

Lepton flavor conservation differs from other conservation laws in the Standard Model (SM) because it is not associated with an underlying conserved current symmetry. While forbidden in the Standard Model (SM), many extensions to the SM predict enhanced LFV in tau decays with respect to muon decays with branching fractions from 10^{-10} up to the current experimental limits [5]. Observation of LFV in tau decays would be a clear signature of physics beyond the SM, while non-observation will provide further constraints on theoretical models.

3.1. $\tau^\pm \rightarrow e^\pm\gamma$ [6]

Events with two or four well-reconstructed tracks inconsistent with coming from a photon conversion are selected. The signal-side hemisphere is required to contain at least one γ with a CM energy greater than 500 MeV, and one track identified as an electron. Backgrounds arising from radiation are reduced by requiring that the total CM energy of all non-signal γ candidates in the signal-side hemisphere be less than 200 MeV. To suppress non- τ backgrounds with significant radiation along the beam directions, the polar angle (θ_{miss}) of the missing momentum associated with the neutrino(s) in the event is required to lie within the detector acceptance ($-0.76 < \cos\theta_{miss} < 0.92$). A correlation between the missing momentum (m_ν^2) and the scaled missing transverse momentum (p_{miss}^T/\sqrt{s}) in the non- τ backgrounds is used to suppress them.

The resolution of the $e\gamma$ mass is improved by assigning the point of closest approach of the e track to the e^+e^- collision axis as the origin of the γ candidate and by using a kinematic fit with $E_{e\gamma}$ constrained to $\sqrt{s}/2$. The resulting energy-constrained mass (m_{EC}) and $\Delta E = E_{e\gamma} - \sqrt{s}/2$ are independent variables apart from small correlations arising from initial and final state radiation. We optimize the selection to obtain the smallest expected upper limit 90% CL in a background-only hypothesis for observing events inside a $\pm 2\sigma$ rectangular box signal box defined by: $|\Delta E - \langle \Delta E \rangle| < 2\sigma(\Delta E)$ and $|m_{EC} - m_\tau| < 2\sigma(m_{EC})$, as shown in Fig. 3.

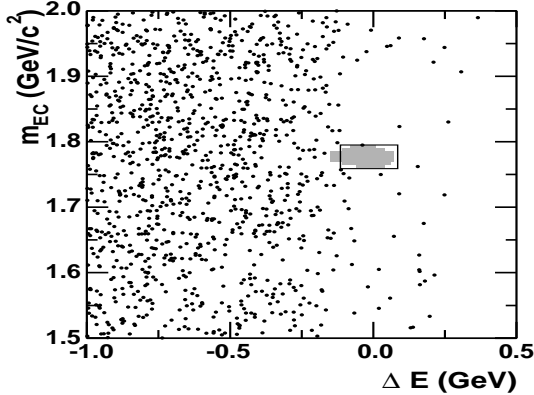


Figure 3. m_{EC} vs. ΔE distribution of data (dots) and shaded region containing 50% of the selected signal MC events inside the Grand Signal Box, as defined in the text. The boundary of the $\pm 2\sigma$ signal box is also shown.

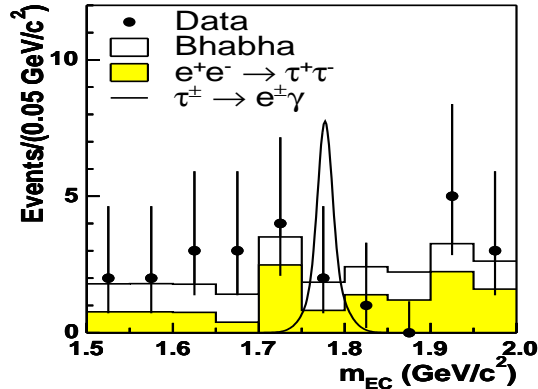


Figure 4. m_{EC} distribution of data (dots), the expected backgrounds (histograms) and MC signal (curve with arbitrary normalization) for $|\Delta E - \langle \Delta E \rangle| < 2\sigma$.

After selection, 8.9% of the total generated MC signal events survive within a Grand Signal Box (GSB) region defined as $m_{\text{EC}} \in [1.5, 2.0]$ GeV/c^2 ,

$\Delta E \in [-1.0, 0.5]$ GeV .

For the final background estimate we use the m_{EC} distribution of data events inside the $\pm 2\sigma(\Delta E)$ band, as shown in Fig. 4 along with the signal shape included for illustrative purposes. We find one event in the signal box for an expected background of 1.9 ± 0.4 events. We set an upper limit employing the same technique used in our search for $\tau^\pm \rightarrow \ell^\pm \ell^+ \ell^-$ [7] where the background levels were also small. This procedure gives an upper limit of $\mathcal{B}(\tau^\pm \rightarrow \mu^\pm \gamma) < 6.0 \times 10^{-8}$ at 90% CL.

3.2. $\tau^\pm \rightarrow \mu^\pm \gamma$ [8]

The analysis follows the broad lines of the $\tau^\pm \rightarrow e^\pm \gamma$ analysis with the difference that it separates the tag-side decays into six categories according to the number of tracks, lepton identification and photon energy. A neural net is then constructed to reduce backgrounds in each category with five observables used as input: the missing mass of the event, the highest CM momentum of the tag-side track(s), μ helicity angle, missing transverse momentum and the invariant mass squared of the missing neutrino.

To obtain the branching ratio, we perform an extended unbinned ML fit to the m_{EC} data distribution (Fig. 5) after all requirements but that on m_{EC} have been applied. The signal efficiency is $(9.4 \pm 0.6)\%$. The fit gives $\mathcal{B}(\tau^\pm \rightarrow \mu^\pm \gamma) = (-5.6^{+8.3}_{-6.3}) \times 10^{-8}$, which corresponds to $-2.2^{+3.2}_{-2.4}$ signal and 143 ± 12 background events. In keeping with established $\tau^\pm \rightarrow \mu^\pm \gamma$ studies, we derive a frequentist upper limit at 90% CL of $\mathcal{B}(\tau^\pm \rightarrow \mu^\pm \gamma) < 6.8 \times 10^{-8}$.

3.3. $\tau^- \rightarrow l^+ l^- l^+$ [7]

The data sample consists of 81.9 fb^{-1} recorded at $\sqrt{s} = 10.58 \text{ GeV}$ and 9.6 fb^{-1} recorded at $\sqrt{s} = 10.54 \text{ GeV}$. Candidate signal events consist of one tau decay yielding three charged particles, while the second tau decay yields one charged particle. All possible lepton combinations consistent with charge conservation are considered, leading to six distinct decay modes.

To reduce backgrounds further, signal events are required to have an invariant mass and total energy in the 3-prong hemisphere consistent

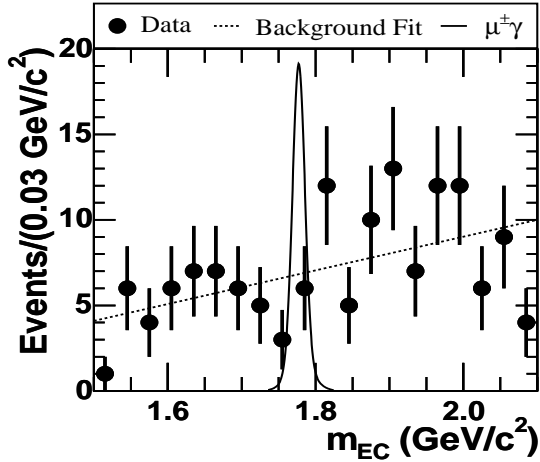


Figure 5. m_{EC} distribution of data (dots), the background component of the fit (dotted line) and MC signal (curve with arbitrary normalization) for $|\Delta E - \langle \Delta E \rangle| < 2\sigma$.

with a parent tau lepton. These quantities are calculated from the observed track momenta assuming the corresponding lepton masses for each decay mode. The energy difference is defined as $\Delta E \equiv E_{\text{rec}}^* - E_{\text{beam}}^*$, where E_{rec}^* is the total energy of the tracks observed in the 3-prong hemisphere and E_{beam}^* is the beam energy, both in the CM frame. The mass difference is defined as $\Delta M \equiv M_{\text{rec}} - m_{\tau}$ where M_{rec} is the reconstructed invariant mass of the three tracks and $m_{\tau} = 1.777 \text{ GeV}/c^2$ is the tau mass.

The expected background rates for each decay mode are determined by fitting a set of probability density functions (PDFs) to the observed data in the $(\Delta M, \Delta E)$ plane in a grand sideband (GSB) region which is defined as the rectangle bounded by the points $(-600 \text{ MeV}/c^2, -700 \text{ MeV})$ and $(400 \text{ MeV}/c^2, 400 \text{ MeV})$, excluding the signal region.

The numbers of events observed (N_{obs}), the background expectations (N_{bgd}) and 90% CL upper limits are shown in Table 1, with no significant excess found in any decay mode.

Table 1

Summary of efficiency estimates, the number of background events (N_{bgd}), the number of observed events (N_{obs}), and the 90% CL upper limit on the branching fraction for each decay mode.

Mode	Efficiency [%]	N_{bgd}	N_{obs}	UL
$e^-e^+e^-$	7.3 ± 0.2	1.51 ± 0.11	1	$2.0 \cdot 10^{-7}$
$\mu^+e^-e^-$	11.6 ± 0.4	0.37 ± 0.08	0	$1.1 \cdot 10^{-7}$
$\mu^-e^+e^-$	7.7 ± 0.3	0.62 ± 0.10	1	$2.7 \cdot 10^{-7}$
$e^+\mu^-\mu^-$	9.8 ± 0.5	0.21 ± 0.07	0	$1.3 \cdot 10^{-7}$
$e^-\mu^+\mu^-$	6.8 ± 0.4	0.39 ± 0.08	1	$3.3 \cdot 10^{-7}$
$\mu^-\mu^+\mu^-$	6.7 ± 0.5	0.31 ± 0.09	0	$1.9 \cdot 10^{-7}$
$e^-K^+K^-$	3.77 ± 0.16	0.22 ± 0.06	0	$1.4 \cdot 10^{-7}$
$e^-K^+\pi^-$	3.08 ± 0.13	0.32 ± 0.08	0	$1.7 \cdot 10^{-7}$
$e^-\pi^+K^-$	3.10 ± 0.13	0.14 ± 0.06	1	$3.2 \cdot 10^{-7}$
$e^-\pi^+\pi^-$	3.30 ± 0.15	0.81 ± 0.13	0	$1.2 \cdot 10^{-7}$
$\mu^-K^+K^-$	2.16 ± 0.12	0.24 ± 0.07	0	$2.5 \cdot 10^{-7}$
$\mu^-K^+\pi^-$	2.97 ± 0.16	1.67 ± 0.29	2	$3.2 \cdot 10^{-7}$
$\mu^-\pi^+K^-$	2.87 ± 0.16	1.04 ± 0.18	1	$2.6 \cdot 10^{-7}$
$\mu^-\pi^+\pi^-$	3.40 ± 0.19	2.99 ± 0.41	3	$2.9 \cdot 10^{-7}$
$e^+K^-K^-$	3.85 ± 0.16	0.04 ± 0.04	0	$1.5 \cdot 10^{-7}$
$e^+K^-\pi^-$	3.19 ± 0.14	0.16 ± 0.06	0	$1.8 \cdot 10^{-7}$
$e^+\pi^-\pi^-$	3.40 ± 0.15	0.41 ± 0.10	1	$2.7 \cdot 10^{-7}$
$\mu^+K^-K^-$	2.06 ± 0.11	0.07 ± 0.10	1	$4.8 \cdot 10^{-7}$
$\mu^+K^-\pi^-$	2.85 ± 0.16	1.54 ± 0.25	1	$2.2 \cdot 10^{-7}$
$\mu^+\pi^-\pi^-$	3.30 ± 0.18	1.46 ± 0.27	0	$0.7 \cdot 10^{-7}$

3.4. $\tau^- \rightarrow l^\mp h^\pm h'^-$ [9]

Candidate signal events are required to have a 1-3 topology, where one tau decay yields one charged particle (1-prong), while the other tau decay yields three charged particles (3-prong). One of the charged particles found in the 3-prong hemisphere must be identified as either an electron or muon candidate. The $(\Delta M, \Delta E)$ quantities and the expected background rates are calculated as for the $\tau^- \rightarrow l^+l^-l^+$ [7] (see above). Rectangular signal regions are defined separately for each decay mode in the $(\Delta M, \Delta E)$ plane.

The numbers of events observed (N_{obs}), the background expectations (N_{bgd}) and the 90% CL upper limits are shown in Table 1, with no significant excess observed.

3.5. $e^-e^+ \rightarrow \tau^\pm l^\mp$

The signature of the signal process in the CM frame is an isolated high-momentum muon or electron recoiling against either one or three charged pions and no neutral particles. The reconstructed mass of the missing neutrino should

be consistent with a massless particle and the invariant mass of the recoiling pions and neutrino consistent with that of the τ .

After the application of these selection criteria, the signal MC reconstruction efficiencies and their statistical error for $\mu^+\tau^-$ are $(18.5 \pm 0.2)\%$ for $\tau^- \rightarrow \pi^-\pi^+\pi^-\nu_\tau$ and $(9.62 \pm 0.14)\%$ for $\tau^- \rightarrow \pi^-\nu_\tau$; for $e^+\tau^-$ they are $(11.73 \pm 0.15)\%$ for $\tau^- \rightarrow \pi^-\pi^+\pi^-\nu_\tau$ and $(11.9 \pm 0.15)\%$ for $\tau^- \rightarrow \pi^-\nu_\tau$.

The backgrounds are dominated by $e^+e^- \rightarrow \tau^+\tau^-$ decays where one τ decays to an e^+/μ^+ plus neutrinos and the other to either $\pi^-\pi^+\pi^-\nu_\tau$ or $\pi^-\nu_\tau$. Light quark continuum processes are predicted to contribute significantly to $e^+e^- \rightarrow \mu^+\tau^-$ ($\tau^- \rightarrow \pi^-\pi^+\pi^-\nu_\tau$) only and events from $e^+e^- \rightarrow \mu^+\mu^-$ are only present in $e^+e^- \rightarrow \mu^+\tau^-$ ($\tau^- \rightarrow \pi^-\nu_\tau$). All other backgrounds are negligible.

An extended unbinned ML fit to the reconstructed τ mass m_τ and e^+/μ^+ CM momentum p_l^* is used to extract the total number of signal and background events separately for each mode. The measurements are not statistically different from the null hypothesis. Preliminary results for the central values of the signal yields from the ML fit and the upper limits on the cross sections and cross section ratios are given in Table 2.

Table 2
Preliminary central values and 95% CL for the signal yields, cross sections and ratio of cross sections to dimuon cross section.

$e^+e^- \rightarrow \mu^+\tau^-$	$\tau^- \rightarrow \pi^-\pi^+\pi^-\nu_\tau$	$\tau^- \rightarrow \pi^-\nu_\tau$
Events	$-1.37 \pm 9.9 \pm 2.6$	$1.9 \pm 10.1 \pm 4.4$
$\sigma_{\mu\tau}$ (fb)	$-0.35 \pm 2.6 \pm 0.7$	$0.85 \pm 4.5 \pm 2.0$
$\sigma_{\mu\tau}$ (fb)	< 5.91	< 11.4
$\sigma_{\mu\tau}/\sigma_{\mu\mu}$	$< 5.2 \times 10^{-6}$	$< 10.1 \times 10^{-6}$
$e^+e^- \rightarrow e^+\tau^-$	$\tau^- \rightarrow \pi^-\pi^+\pi^-\nu_\tau$	$\tau^- \rightarrow \pi^-\nu_\tau$
Events	$15.9 \pm 10.3 \pm 2.7$	$10.7 \pm 8.8 \pm 2.7$
$\sigma_{e\tau}$ (fb)	$6.5 \pm 4.2 \pm 1.1$	$3.9 \pm 3.2 \pm 1.0$
$\sigma_{e\tau}$ (fb)	< 14.8	< 11.1
$\sigma_{e\tau}/\sigma_{\mu\mu}$	$< 13.1 \times 10^{-6}$	$< 9.8 \times 10^{-6}$

We combine the $\tau^- \rightarrow \pi^-\pi^+\pi^-\nu_\tau$ and $\tau^- \rightarrow \pi^-\nu_\tau$ decays and calculate 95% CL upper limits on the cross sections of < 4.6 fb for $e^+e^- \rightarrow \mu^+\tau^-$

and < 10.1 fb for $e^+e^- \rightarrow e^+\tau^-$. The 95% CL upper limits on the ratio of the cross sections with respect to the dimuon cross section are calculated to be $\sigma_{\mu\tau}/\sigma_{\mu\mu} < 4.0 \times 10^{-6}$ and $\sigma_{e\tau}/\sigma_{\mu\mu} < 8.9 \times 10^{-6}$.

4. The Future and Acknowledgments

By the end of their data-taking, the current generation of B -meson factories will have produced over 2 billion τ pair decays. The physics potential of this legacy has only just begun to be exploited.

We are grateful for the excellent luminosity and machine conditions provided by our PEP-II colleagues, and for the effort from the computing organizations that support BABAR. The collaborating institutions wish to thank SLAC for its support. This work is supported by DOE and NSF (USA), NSERC (Canada), IHEP (China), CEA and CNRS-IN2P3 (France), BMBF and DFG (Germany), INFN (Italy), FOM (The Netherlands), NFR (Norway), MIST (Russia), and PPARC (United Kingdom). Individuals have received support from CONACyT (Mexico), Marie Curie EIF (European Union), the A. P. Sloan Foundation, the Research Corporation, and the Alexander von Humboldt Foundation.

REFERENCES

1. BABAR Collaboration, B. Aubert *et al.*, Nucl. Instr. Methods Phys. Res., Sect. A **479**, 1 (2002).
2. BABAR Collaboration, B. Aubert *et al.*, Phys. Rev. **D72**, 072001 (2005).
3. S. Jadach, Z. Was, R. Decker, and J. H. Kuhn, Comput. Phys. Commun. **76**, 361 (1993).
4. BABAR Collaboration, B. Aubert *et al.*, Phys. Rev. **D72**, 012003 (2005).
5. E. Ma, Nucl. Phys. B Proc. Suppl. **123**, 125 (2003).
6. BABAR Collaboration, B. Aubert *et al.*, Phys. Rev. Lett. **96**, 041801 (2006).
7. BABAR Collaboration, B. Aubert *et al.*, Phys. Rev. Lett. **92**, 121801 (2004).
8. BABAR Collaboration, B. Aubert *et al.*, Phys. Rev. Lett. **95**, 041802 (2006).
9. BABAR Collaboration, B. Aubert *et al.*, Phys. Rev. Lett. **95**, 191801 (2005).